Effect of robust torus on the dynamical transport

2010 J. Phys.: Conf. Ser. 246 012005

(http://iopscience.iop.org/1742-6596/246/1/012005)

Effect of robust torus on the dynamical transport

Caroline G. L. Martins[1], R. Egydio de Carvalho[1], I. L. Caldas[2] and M. Roberto[3]

[1] UNESP-Univ Estadual Paulista; Instituto de Geociências e Ciências Exatas; Departamento de Estatística, Matemática Aplicada e Computação, Av. 24A, 1515, 13506-900 Rio Claro , SP, Brazil.
[2] Universidade de São Paulo; Instituto de Física 05315-970 São Paulo, SP, Brazil.
[3] Instituto Tecnológico da Aeronáutica; Departamento de Física 12228-900 São José dos Campos, SP, Brazil.

E-mails: carolinegameiro@gmail.com, regydio@rc.unesp.br, ibere@if.usp.br,

marisar@ita.br

Abstract In the present work, we quantify the fraction of trajectories that reach a specific region of the phase space when we vary a control parameter using two symplectic maps: one non-twist and another one twist. The two maps were studied with and without a robust torus. We compare the obtained patterns and we identify the effect of the robust torus on the dynamical transport. We show that the effect of meandering-like barriers loses importance in blocking the radial transport when the robust torus is present.

1. Introduction

In a previous work [1] we introduced a non-twist map with a new transport barrier called robust torus (RT), through a known Hamiltonian derivation in which the RT had been introduced in a systematic way [2,3,4]. The motivation to create this new map was the relevance of transport barrier to plasma confinement in tokamaks [5-7] and also because our map could be a natural extension of usual maps [8-13] applied to study theoretically transport in tokamaks. In another work [14] we adapted our map with a single robust torus and adjusted the parameters according to the experimental ones used in the tokamak TCABR. We have verified that the RT regularizes the orbits close to its position in the phase space and blocks the radial transport inside the tokamak plasma. The main idea to create a RT is to introduce an appropriate polynomial pre-factor multiplying the resonant perturbations which act on the system in such way that their effects vanish on particular positions of the phase space even if the control parameter is turned on. This vanishing will occur in the values of the roots of the pre-factor. The RT in fact corresponds to an invariant curve which remains intact under the action of any generic perturbation.

In this work, we quantify the portion of trajectories that reach a specific region of the phase space when we vary a control parameter using two maps: one non-twist and another twist, both of them with or without a robust torus. The non-twist maps present isochronous resonances [15], which can reconnect themselves and generate the well known meandering barriers [16].

We compare the obtained patterns for the non-twist and twist maps, with and without RT, and we identify the effect of the RT on the dynamical transport. We create a RT near a secondary resonant mode and we show that the robustness of the RT is transferred to its neighborhood. Because

of that, the effect of the other meandering-like barrier, present in the non-twist map, loses importance in blocking the radial transport when the RT is present.

The paper is organized as follows; in Section 2 we present a brief Hamiltonian approach relevant for plasma confinement in tokamak. In Section 3 we show the corresponding non-linear maps, twist and non-twist, which we are going to use. In Section 4 we discuss the results on transport in the phase space and in last section we present final remarks.

2. Hamiltonian Approach

As a background motivation, in this section we review the usual Hamiltonian approach developed for plasma confinement in tokamaks in order to introduce the RT in this formalism and also to link it with our map. We propose an equilibrium Hamiltonian, H_0, with toroidal symmetry and we define the toroidal angle, φ, as the canonical time t. This non-perturbed Hamiltonian corresponds to an integrable system and it is described by an analytical solution of the non-linear Grad-Shafranov equation [17]. H_0 is given in terms of the action J, corresponding to the toroidal normalized flux, and ϑ the poloidal angle canonically associated to J [18]. The perturbations are generated by a helical electric current applied from thins ergodic magnetic limiters (EML) distributed along the poloidal direction in toroidal sections of the tokamak [19]. The perturbing Hamiltonian, H_1, is a function of J, ϑ and t, and it is represented by a Fourier expansion of delta-kicks due to the EML rings [10]. The perturbations create a region with chaotic magnetic field lines at the plasma edge.

We expand H_0 around a magnetic surface with action J_0 and frequency $\Omega_0=n/m$ where Ω_0 is equal to the inverse of the safety factor q and *n* and *m* are integers. In the Fourier perturbation expansion, we keep only the two main resonances in such way the Hamiltonian has only the dominant resonant modes with poloidal wave numbers *m* and *(m+1)* [10,19],

$$H(\Delta J,\vartheta,t) = H_0(\Delta J) + P(\Delta J)[\beta\cos(m\vartheta)+\eta\cos((m+1)\vartheta+nt)]\sum_{k=-\infty}^{+\infty}\delta\left(t-\frac{2\pi}{N_r}k\right) \qquad (1)$$

where $\Delta J = J - J_0$ and $N_r=4$ is the quantity of EML rings equally spaced around the tokamak.

We also consider two equilibrium configurations for the frequency profiles $\Omega_0 \equiv dH_0/d\Delta J$ given by:

$$H_0(\Delta J)=\frac{1}{2}\Delta J^2 \qquad (2)$$

for the twist case and

$$H_0(\Delta J)=\frac{1}{2}\Delta J^2-\frac{\alpha}{3}\Delta J^3 \qquad (3)$$

for the non-twist case.

The parameters β and η in Eq. (1) represent the perturbing electric current applied in EML rings and the parameters α in Eq. (3) is determined by the safety factor profile defined by H_0. The pre-factor *P(ΔJ)* in Eq. (1) is a polynomial function and it allows us to introduce the RT.

We emphasize that, for a generic polynomial function, it is possible to have a number of RT equal to the number of real roots of this polynomial. Thus, this procedure enables us to construct a Hamiltonian to study the alterations of the magnetic field lines topology due to the presence of an infinity barrier, a RT.

3. Non-linear maps

In order to investigate the characteristics of the phase space concerning transport, due to the presence of a RT, we consider the Hamiltonian of Eq. (1) with the non-perturbed Hamiltonian, H_0, of Eq. (2) and (3), twist and non-twist cases respectively. We also choose two configurations for the pre-factor, one with $P(\Delta J)=1$ for the usual Hamiltonian without RT and another one with $P(\Delta J)=(\Delta J-a)$ introducing one RT in the position $\Delta J=a$. However, instead of working with the Hamiltonian formulation we will take the corresponding non-linear map associated to the Hamiltonian of Eq. (1) that was derived in details by us in [1]. Thus, the non-twist map with two resonant modes and without RT is,

$$\begin{aligned}
\Delta J_{k+1} &= \Delta J_k + \beta m \sin(m\vartheta_k) + \eta(m+1)\sin[(m+1)\vartheta_k + nt_{k+1}] \\
\vartheta_{k+1} &= \vartheta_k + \frac{2\pi}{N_r}(\Delta J_{k+1} - \alpha \Delta J_{k+1}^2) \quad , \quad \mathrm{mod}(2\pi) \\
t_{k+1} &= t_k + \frac{2\pi}{N_r m}
\end{aligned} \tag{4}$$

The non-twist map with two resonant modes and with one RT is,

$$\begin{aligned}
\Delta J_{k+1} &= \Delta J_k + (\Delta J_{k+1} - a)\{\beta m \sin(m\vartheta_k) + \eta(m+1)\sin[(m+1)\vartheta_k + nt_{k+1}]\} \\
\vartheta_{k+1} &= \vartheta_k + \frac{2\pi}{N_r}(\Delta J_{k+1} - \alpha \Delta J_{k+1}^2) + \beta\cos(m\vartheta_k) + \eta\cos[(m+1)\vartheta_k + nt_{k+1}] \quad , \quad \mathrm{mod}(2\pi) \\
t_{k+1} &= t_k + \frac{2\pi}{N_r m}
\end{aligned} \tag{5}$$

In all numerical calculations we chose $m=3$ and $n=1$ introducing the resonant modes (1:3) and (1:4). The constant α that appears in Eq. (3) is adjusted for both maps, in the twist case $\alpha=0$ and in the non-twist case $\alpha=160.15$. We will split our study in four analyses:
i) Case Non-twist without RT, Eq. (4) with $\alpha=160.15$;
ii) Case Non-twist with one RT, Eq. (5) with $\alpha=160.15$;
iii) Case Twist without RT, Eq. (4) with $\alpha=0$;
iv) Case Twist with one RT, Eq. (5) with $\alpha=0$.

For the non-twist equilibrium, there are isochronous resonances in the phase space. Figure 1(a) corresponds to the case **i)**, where two isochronous resonances (1:3) has already reconnected and they are dimerized and separated by invariant meandering curves. Such invariant curves encircle both sets of surviving islands (1:3) and they exist only in non-twist maps. In plasma confinement approaches, the meandering curves are located in the shearless region, which traps the magnetic field lines for a long time hampering the radial diffusion, in such way that an internal transport barrier (ITB) takes place due to a strong stickiness effect [20].

Figure 1(b) corresponds to the case **ii)**, the RT is indicated in blue color at the position $\Delta J=3=a$, and the alterations introduced in the dynamics are noticeable. We still have the two *(1:3)* and *(1:4)* island chains, but now an interesting topological rearrangement occurred, the chaotic sea that was close to the upper island chain *(1:4)*, in Figure 1(a), had been suppressed due to the presence of the RT. The motion near the RT is kept integrable while in the other side of the meandering curves there is still a significant destruction of the invariant curves around the low resonance *(1:4)* showing a visible chaotic sea.

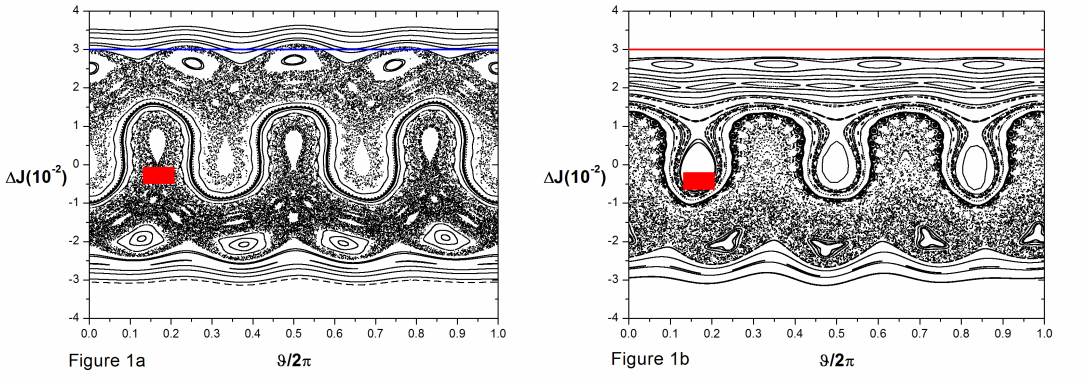

Figure.1. Poincaré sections for the resonant modes (1:3) and (1:4) for α=160.15: **(a)** Non-twist map, Eq. (4), without RT with $\beta = -1.3\text{x}10^{-4}$ and $\eta = 1.15x10^{-4}$, the blue line at ΔJ=3 is only to guide the eyes, it is not a RT; **(b)** Non-twist map, Eq. (5), with RT (in red) at ΔJ=3, with $\beta = -4.0\text{x}10^{-3}$ and $\eta = 9.2\text{x}10^{-3}$.

Figure 2(a) corresponds to the case **iii)** and we see the dominant island chain (1:3) and the main secondary resonance (1:4) embedded in a chaotic sea with several other secondary resonances. In this configuration, the barriers are in fact the island structures, which will be destroyed as the parameters are varied. On the other hand, in Figure 2(b), which corresponds to the case **iv)**, we can see the stabilizing alterations introduced by the RT, which is indicated in red colour in *ΔJ=a=3*. Note that, for the parameters used to plot Figure 2(b), the chaotic sea near the RT, around the island (1:3), is suppressed and the neighbourhood around *ΔJ=3* is more stable than the one of the Figure 2(a) evidencing the local effect of the RT.

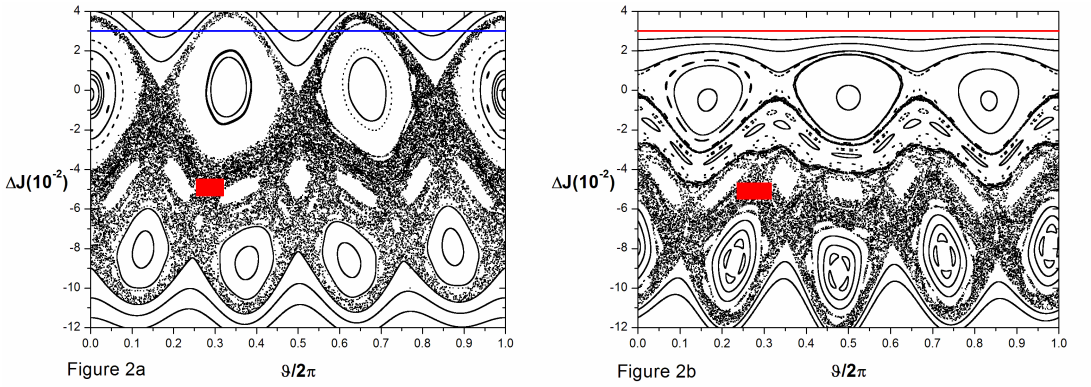

Figure.2. Poincaré sections for the resonant modes (1:3) and (1:4) with α=0 for: **(a)** Twist map, Eq. (4), without RT with $\beta = -6.0\text{x}10^{-4}$ and $\eta = 2.99\text{x}10^{-4}$, the blue line at ΔJ=3 is only to guide the eyes, it is not a RT. **(b)** Twist map, Eq.(5), with RT (in red) at ΔJ=3, with $\beta = -7.5\text{x}10^{-3}$ and $\eta = 8.2\text{x}10^{-3}$.

We should emphasize that different Hamiltonians (maps) govern the system without RT (Figures 1(a) and 2(a)) and with RT (Figures 1(b) and 2(b)) and hence the scale of the parameters are different. In addition, the ranges of β are different because the non-twist system has one term that does not appear in the twist system.

4. Dynamical transport on the phase space

In this section we present the transport of an ensemble of initial conditions given inside the small red boxes in Figures 1 and 2, with and without RT, as function of the parameter β. We iterated 110 initial conditions inside the red squares and we varied the perturbation parameter β in order to investigate how many initial conditions reach the position $\Delta J=3$ (in blue), after 2500 iterations of the maps of equations (4) and (5). This small quantity of collected iterations does not lead to any loss of generality because we intend to investigate the effect of barriers or stickiness in the transport, which could be neglected if we had taken a bigger quantity of iterations than the one considered here.

For the non-twist cases, the meandering curves play the role of partial barrier and they interfere differently on the transport depending on the presence of the RT. When the system does not have a RT, case **i)**, the trajectories reach the reference line after the destruction of the meandering curves. However, as showed in [21] this kind of curves has a discontinuous behaviour, they disappear for some values of β but they exist for many other intercalated values of β. So, for the case i) without RT, the fluctuations seen in Figure 3(a) show exactly the sensibility of the meandering curves for different values of the perturbation, while for the case ii) with a RT, in Figure 3(b) the trajectories reach the reference line, which is in fact the RT, only after the destruction of the resonance mode (1:4). Hence, in this case, the destruction or existence of the meandering curves is not a sufficient condition for the considered orbits reach the reference position. For the twist case, the small boxes in Figures 1 and 2 are above the resonance (1:4), thus we are going to investigate the effect of the RT in the neighborhood of the resonance mode (1:3). Figure 3(c) and 3(d) correspond to the case **iii)** and **iv)** respectively, and we observe a similar behaviour in the transport rates but with a small nuance. In the case without RT, Figure 3(c), as the structures are being destroyed the transport increases but the trajectories still find some regions with a soft stickiness. In the case with RT, Figure 3(d), as the resonance structures are destroyed the transport increases abruptly and we observe a soft stickiness only around the RT.

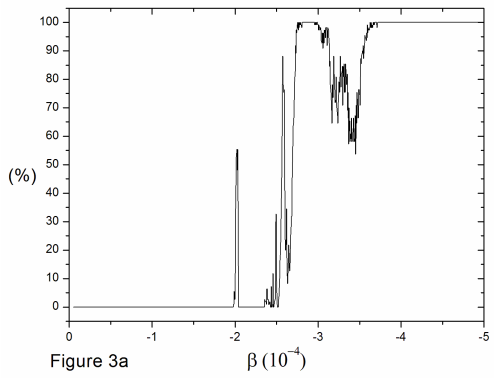

Figure 3a

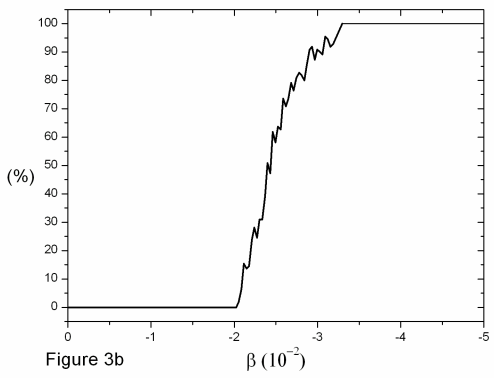

Figure 3b

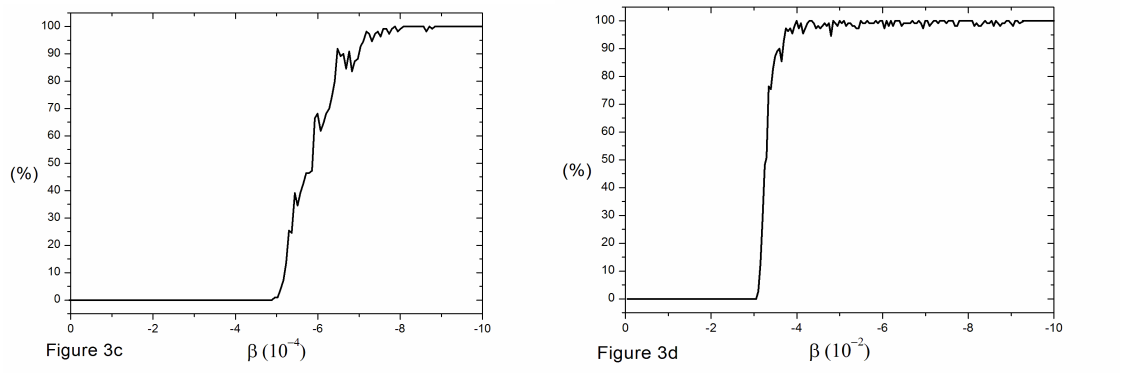

Figure.3. Percentage of initial conditions that arrived $\Delta J=3$ up 2500 iterations: **(a)** Non-twist map without RT, Eq. (4); **(b)** Non-twist map with RT, Eq. (5); **(c)** Twist map without RT, Eq. (4); **(d)** Twist map with RT, Eq. (5).

5. Conclusions

The non-liner maps that we use here may describe the equilibrium magnetic field lines perturbed by resonances created by rings of ergodic magnetic limiters. In previous works [1,14], robust torus had proved to be, theoretically, an efficient transport barrier that prevented the magnetic field lines to reach the tokamaks wall, avoiding plasma-wall interactions.

We showed here the behavior of two different transport barriers, one formed by the reconnection process of isochronous resonances, the meandering curves, and another formed by the vanishing of the perturbation in a particular region, through the introduction of a RT. In our approach the RT is stronger than the meandering barriers due to the stabilizing effect it induces in its neighborhood. We checked the behaviour of dynamical transport from our maps for different resonant modes with rotation number close to the resonant mode (1:3) used here, and we have observed that the qualitative behavior of the transport is similar with the plots showed in figure (3). The RT plays a remarkable influence on the dynamical transport; this is the reason that this kind of robust barrier is relevant for Hamiltonian plasma approaches.

Acknowledgments

The authors thank the scientific Brazilian agencies FAPESP and CNPQ for financial support.

References

[1] Martins C G L, Egydio de Carvalho R, Caldas I L, Roberto M 2010 *J. Phys. A* to appear
[2] Voyatzis G and Ichtiaroglou S 1999 *Int. J. Bif. and Chaos* **9**(5) 849
[3] Egydio de Carvalho R and Favaro G M 2005 *Physica A* **350** 173
[4] Egydio de Carvalho R, Martins C G L and Favaro G M 2009 *Braz. J. Phys.* **39**(3) 606
[5] Horton W 1999 *Rev. Mod. Phys.* **71** 735
[6] Wolf R C 2003 *Plasma Phys. Control. Fusion* **45** R1
[7] Connor J W et al 2004 *Nucl. Fusion* **44** R1
[8] Portela J S E, Caldas I L, Viana R L 2008 *Eur. Phys. J. Special Topics* **165** 195
[9] Roberto M, da Silva E C, Caldas I L, Viana R L 2004 *Braz. J. Phys.* **34(4B)** 1769
[10] Roberto M, da Silva E C, Caldas I L, Viana R L 2004 *Physica A* **342** 363
[11] Roberto M, da Silva E C, Caldas I L and Viana R L 2004 *Phys. Plasma* **11(1)** 214.
[12] Wurm A, Apte A and Morrison P J 2004 *Braz. J. Phys.* **34(4B)** 1700.
[13] Caldas I L, Viana R L, Araújo M S T, Vannucci A, da Silva E C, Ullmann K and Heller M V A P 2002 *Braz. J. Phys.* **32(4)** 980.
[14] Martins C G L, Egydio de Carvalho R, Caldas I L, Roberto M 2010 submitted

[15] Egydio de Carvalho R and Ozório de Almeida A M 1992 *Phys. Lett. A* **162** 457
[16] Wurm A, Apte A, Fuchss K and Morrison P J 2005 *Chaos* **15** 023108
[17] Kucinski M Y and Caldas I L 1987 *Z. Naturforsch A: Phys. Sci* **42** 1124.
[18] Roberto M, Silva E C, Caldas I L and Viana R L 2005 *J. Phys.:Conf. Series* **7** 163
[19] Karger F and Lackner F 1975 *Phys. Lett. A* **61(6)** 385
[20] Szezech J D, Caldas I L, Lima G Z S, Viana R L, Morrison P J 2009 *Chaos* **19** 043108
[21] Morrison P J 2000 *Phys. Plasma* **7(6)** 2279